DOI:10.1002/ejic.201301098

Highly Selective H_2O_2-Based Oxidation of Alkylphenols to *p*-Benzoquinones Over MIL-125 Metal–Organic Frameworks

Irina D. Ivanchikova,[a] Ji Sun Lee,[b,c] Nataliya V. Maksimchuk,[a] Alexander N. Shmakov,[a] Yurii A. Chesalov,[a] Artem B. Ayupov,[a] Young Kyu Hwang,[b] Chul-Ho Jun,[c] Jong-San Chang,*[b,d] and Oxana A. Kholdeeva*[a]

Keywords: Heterogeneous catalysis / Oxidation / Hydrogen peroxide / Metal–organic framework / Titanium

The titanium-based metal–organic framework MIL-125 and its amine-functionalized analog, MIL-125_NH$_2$, have been synthesized and characterized by elemental analysis, XRD, SEM, TEM, N_2 adsorption measurements, and spectroscopic techniques, including FTIR, Raman, and DR UV/Vis spectroscopy. Catalytic properties of MIL-125 and MIL-125_NH$_2$ were evaluated in the selective oxidation of two representative alkyl-substituted phenols, 2,3,6-trimethylphenol and 2,6-di-*tert*-butylphenol, with the clean oxidant H_2O_2. With both MIL-125 and MIL-125_NH$_2$, the selectivity toward the corresponding *p*-benzoquinones was 100 %. Samples of MIL-125 with different sizes of crystallites (0.5, 1.5, and 5 µm) demonstrated similar reaction rates, thus indicating the absence of diffusion limitations. The efficiency of the oxidant utilization and stability of the MIL-125 structure increased upon decreasing the amount of water in the reaction mixture. Even if the structural integrity of MIL-125 was destroyed by the reaction medium, the metal–organic framework acted as a precursor for the highly active, selective, and recyclable catalyst. The MIL-125-derived materials were stable toward titanium leaching, behaved as true heterogeneous catalysts, and could easily be recovered by filtration and reused several times without the loss of the catalytic properties.

Introduction

Metal–organic frameworks (MOFs) are functional porous coordination polymers with a crystalline structure comprised of metal ions or clusters linked by polydentate organic ligands. Because of their unique combination of properties, such as large surface areas and pore volumes, diverse topologies, and possibilities of functionalization, MOFs have generated a great deal of interest in recent years as prospective materials for gas or liquid adsorption and separation, molecular recognition, and heterogeneous catalysis.[1] Moreover, MOFs can be applied as precursors for the preparation of various nanomaterials.[2]

An important feature of MOFs is a high content of metal sites (most often, well-defined clusters), which are uniformly spatially distributed and are accessible for reagents. Titanium is a very attractive candidate for construction of MOFs due to its low toxicity, photocatalytic activity, and potential ability to activate hydroperoxides. Ti-containing solids, in particular, titanium-silicates are well known as effective catalysts for a number of selective oxidations with aqueous hydrogen peroxide and alkylhydroperoxides.[3] Recently, Férey and coworkers reported on the synthesis of a titanium-oxo-hydroxo-cluster-based MOF designated as MIL-125 using terephthalic acid (H_2bdc) and titanium(IV) isopropoxide.[4] The quasi-cubic tetragonal structure of MIL-125 is built up from cyclic octamers of edge- and corner-sharing $TiO_5(OH)$ octahedra connected to 12 other cyclic octamers through 1,4-benzenedicarboxylate (bdc) linkers. The structure of MIL-125 has two types of cages, namely, an octahedral one (12.5 Å diameter) and a tetrahedral one (6 Å diameter), accessible through triangular windows of 5–7 Å. An amine-functionalized analog MIL-125_NH$_2$, isostructural to MIL-125, has been prepared by replacing H_2bdc with 2-amino benzene dicarboxylic acid (H_2bdc-NH$_2$).[5] Photocatalytic properties of MIL-125 and MIL-125_NH$_2$ were studied by a few research groups.[4–6] Kim et al. demonstrated the catalytic activity of both Ti-

---

[a] Boreskov Institute of Catalysis,
Pr. Akademika Lavrentieva 5, Novosibirsk 630090, Russia
E-mail: khold@catalysis.ru
www.catalysis.ru
[b] Korea Research Institute of Chemical Technology (KRICT),
P. O. Box 107, Gajeongro 141, Yuseong, Daejeon 305-600, Republic of Korea
E-mail: jschang@krict.re.kr
http://rgn.krict.re.kr/index.sko
[c] Department of Chemistry and Center for Bioactive Molecular Hybrid, Yonsei University, Seoul 120-749, Republic of Korea
[d] Department of Chemistry, Sungkyunkwan University, Suwon 440-476, Republic of Korea

Supporting information for this article is available on the WWW under http://dx.doi.org/10.1002/ejic.201301098.

MOFs in high-pressure cycloaddition of CO_2 to epichlorohydrin.[7] They also studied the oxidative desulfurization of heterocyclic aromatic sulfur compounds with cumene hydroperoxide over MIL-125.[7] Recently, McNamara et al. reported similar results using *tert*-butyl hydroperoxide (TBHP) as the oxidant.[8] To the best of our knowledge, no examples have been reported to date on the application of MIL-125 in H_2O_2-based liquid-phase oxidation.

The selective oxidation of substituted phenols is a topic of great interest since quinones bearing different functional groups are intermediates in the production of fine chemicals, including the synthesis of vitamins E and K, coenzyme Q, and other valuable products.[9] Recently, some of us found that Ti,Si catalysts prepared by grafting titanium(IV) onto commercial mesoporous silicas are efficient catalysts for oxidation of 2,3,6-trimethylphenol (TMP) and 2,6-dimethylphenol with H_2O_2 to produce 2,3,5-trimethyl-1,4-benzoquinone (TMBQ, vitamin E key intermediate) and 2,6-dimethyl-1,4-benzoquinone, respectively, with a nearly quantitative yield.[10] A correlation between the selectivity toward quinone and Ti surface concentration has been revealed.[10b,10c] The key point to achieve the high quinone selectivity was found to be the presence of Ti^{IV} dimers or small clusters homogeneously distributed on the silica surface.[10b,10c] Taking into account that the structure of MIL-125 is composed of titanium oxo-hydroxo clusters, one might expect that highly selective oxidation of alkylphenols to *p*-benzoquinones could be realized over this MOF. Following this idea, we explored the catalytic performance of MIL-125 and MIL-125_NH_2 in the oxidation of two representative alkyl-substituted phenols, TMP and 2,6-di-*tert*-butylphenol (DTBP), using aqueous H_2O_2 as the oxidant and acetonitrile as the solvent. The results obtained have been compared with the results acquired using Ti,Si catalysts and anatase. Special attention was drawn to the crucial issues of the catalyst stability and recyclability.

Results and Discussion

Catalyst Preparation and Characterization

MIL-125 was synthesized by a solvothermal method as reported elsewhere.[11] Detailed procedures for the synthesis of MIL-125 and MIL-125_NH_2 are given in the Supporting Information (SI). Samples of MIL-125 with three different sizes of crystallites (0.5, 1.5, and 5.0 µm) have been designated as MIL-125-S, MIL-125-M, and MIL-125-L, respectively. Figure 1 shows SEM images of the MIL-125 and MIL-125_NH_2 samples. MIL-125-M, which was prepared by a conventional procedure, was rather disk-like in shape with crystallites of ca. 1.5 µm, while MIL-125_NH_2 was rather rectangular in shape with particles of ca. 0.7 µm. It was found that benzoic acid and water can be used as a modulator to affect the particle size of MIL-125. The addition of benzoic acid [molar ratio of benzoic acid/Ti(O*i*Pr)$_4$ = 10] leads to smaller crystallites (ca. 0.5 µm, MIL-125-S) while the addition of water [molar ratio of H_2O/Ti(O*i*Pr)$_4$ = 1] favors the formation of larger particles (ca. 5 µm, MIL-125-L).

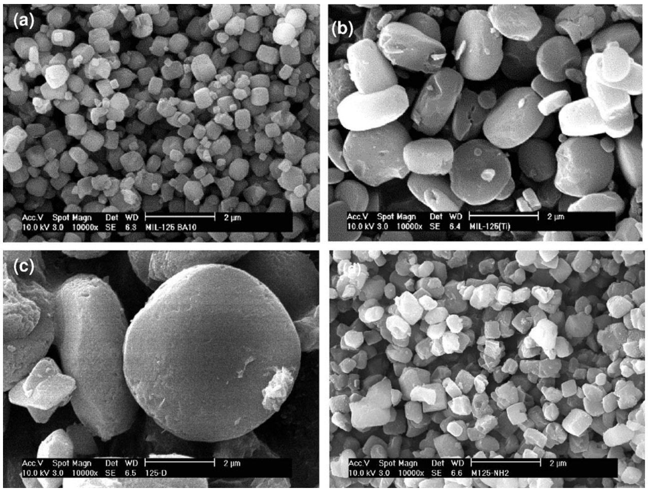

Figure 1. SEM images of (a) MIL-125-S, (b) MIL-125-M, (c) MIL-125-L, and (d) MIL-125_NH_2.

Figure S1 (see SI) shows TG profiles of MIL-125-M and MIL-125_NH_2. Virtually identical TG profiles were obtained for the two samples. On the whole, two weight-loss steps were observed: the first one corresponds to the departure of the guest molecules (H_2O, MeOH, and DMF) over the range 25–300 °C (ca. 35 %) and the second one may be from the phase transition or structure reorganization above 300 °C in MIL-125_NH_2 and 450 °C in MIL-125-M.[11] The first weight loss below 100 °C (ca. 30 %) is attributed to the departure of guest solvents, mainly water, because the samples were fully saturated at 70 % humidity before the TGA measurements.

XRD patterns of MIL-125-M and MIL-125_NH_2 are given in Figure S2 in the SI and confirm the structure of MIL-125 reported by Férey and coworkers.[4] Low-temperature nitrogen adsorption revealed type I isotherms characteristic of microporous solids (Figure S3 in SI, curve A). Textural parameters acquired from the N_2 adsorption measurements are presented in Table 1 along with the elemental analysis data and the average particle size estimated by SEM. Specific BET surface areas exceeded (ca. 10–15 %) the values reported in the literature for MIL-125-M and for MIL-125_NH_2.[4,5,6b] Micropore volumes estimated by the α_S-plot method were close to the value of 0.65 $cm^3 g^{-1}$ reported for MIL-125.[4]

FTIR spectra of MIL-125-M and MIL-125_NH_2 (Figure S4 in SI, curves A) reveal strong characteristic bands arising from asymmetric (1500–1700 cm^{-1}) and symmetric (1350–1450 cm^{-1}) vibrations of carboxylate groups along with O–Ti–O vibrations over the range 400–800 cm^{-1}. No band at 1710 cm^{-1}, characteristic of free H_2bdc, was present corroborating the absence of the free linker within the micropores. Raman spectra of MIL-125-M and MIL-125_NH_2 (Figure 2a and 2b, respectively, curves A) are also consistent with the literature.[6b,11] It is well known that the

Table 1. Physicochemical properties of Ti-MOFs studied.

Catalyst	Ti [wt.-%]	Particle size [µm]	S_{BET} [m^2 g^{-1}]	V_{micro}[a] [cm^3 g^{-1}]	V_{meso}[b] [cm^3 g^{-1}]
MIL-125-S	23.8	0.5	1713	0.64	0
MIL-125-M	20.0	1.5	1868	0.76	0
	25.9[c]		320[c]	0[c]	0.25[c]
	30.0[d]		364[d]	0[d]	0.23[d]
MIL-125-L	24.6	5.0	1683	0.64	0
MIL-125_NH$_2$	23.5	0.7	1575	0.54	0

[a] Micropore volume. [b] Mesopore volume. [c] After one run in TMP oxidation with H_2O_2; reaction conditions as in Table 2, entry 5. [d] After four runs in TMP oxidation with H_2O_2; reaction conditions as in Table 2, entry 5.

Raman technique enables the early detection of the emergence of anatase microcrystallites in Ti-containing solids by the presence of a strong absorption band at 140–145 cm^{-1}.[3c,3f,12] The lack of this absorption (see inserts in Figure 2) in the Raman spectra of both Ti-MOFs confirms that no anatase-like admixtures are present.

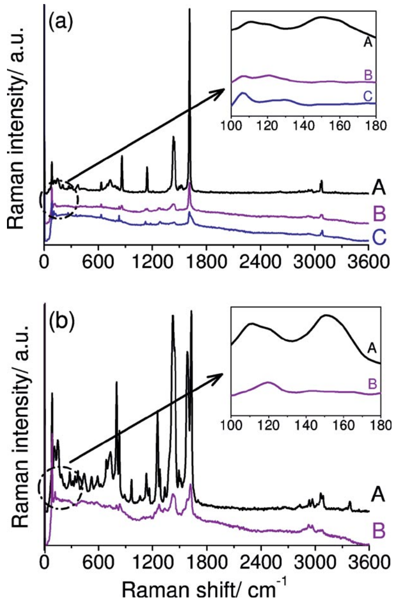

Figure 2. Raman spectra of (a) MIL-125-M and (b) MIL-125_NH$_2$: (A) initial, (B) and (C) after 1 run and 4 runs of TMP oxidation with H_2O_2, respectively. Reaction conditions: TMP (0.1 M), H_2O_2 (0.4 M), MIL-125 (21 mg), MeCN (7 mL), 80 °C, 10 min.

DR UV/Vis spectra of MIL-125-M and MIL-125_NH$_2$ are shown in Figure 3a and 3b, respectively (curves A). The spectra resemble those reported in the literature.[6,7] While MIL-125 shows two main adsorptions with maxima centered at ca. 240 and 290 nm, MIL-125_NH$_2$ reveals an additional band at ca. 390 nm with the absorption edge extending to around 500 nm (Figure 3, b) associated with the chromophore of bdc-NH$_2$ units.[6a] It is well documented in the literature that solids with site-isolated tetrahedrally coordinated Ti^{IV} centers exhibit a narrow absorption band at 208–210 nm attributed to an oxygen-to-metal charge transfer,[3c,3f,12a,13] while the increase in the Ti^{IV} coordination number and the appearance of dimeric and oligomeric TiO_2 species are manifested by a long-wave shift and broadening of the DRS UV/Vis band.[3d,3f,9b,12a,13,14] Figure S5 in the SI shows the DR UV/Vis spectra of the three samples of MIL-125 in comparison with the spectrum of a silica-grafted titanium catalyst (the latter contained well-dispersed oligomeric TiO_2 species).[10b] One can see that the spectra of both types of the Ti catalysts are quite similar. Hence, we might tentatively ascribe the adsorptions at 240 and 290 nm in the DR UV/Vis spectra of MIL-125 to ligand-to-metal charge-transfer bands from the presence of, at least, two types of octahedrally coordinated clusterized Ti^{IV} species.

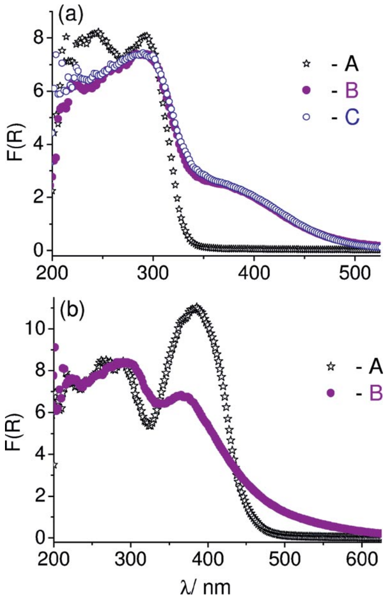

Figure 3. DR UV/Vis spectra of (a) MIL-125-M and (b) MIL-125_NH$_2$: (A) initial, (B) and (C) after 1 and 4 runs of TMP oxidation with H_2O_2, respectively. Reaction conditions as in Figure 2.

Catalytic Properties

Catalytic properties of the MIL-125 materials were first assessed in TMP oxidation with aqueous H_2O_2 in acetonitrile solvent. The main results are collected in Table 2. Both MIL-125 and MIL-125_NH$_2$ favored the formation of TMBQ with 100% selectivity (Table 2, entries 1 and 2). With another substituted phenol, DTBP, the corresponding *p*-benzoquinone was also the sole oxidation product found by means of both GC and ^{1}H NMR spectroscopy, thereby indicating excellent selectivity.

Earlier, some of us established, for titanium-silicate catalysts, that the crucial point to achieve excellent benzoquinone selectivity in the H_2O_2-based oxidation is the presence of Ti^{IV} dimers or small clusters on the silica surface. Such species are manifested by broad DRS UV/Vis bands in the range 240–290 nm (see, for example, curve D in Figure S5 in the SI).[10b,10c] Catalysts that contain isolated Ti^{IV} sites (DRS UV maximum at 210–220 nm) and/or anatase-like microcrystallites (DRS UV/Vis: 330–340 nm) produce a significant amount of dimeric byproducts.[10c,12b] Hence, we can suggest that the outstanding selectivity toward TMBQ

Table 2. TMP oxidation with H_2O_2 over MIL-125.[a]

Entry	Catalyst	$[H_2O_2]$ [M]	TMP conversion [%]	H_2O_2 efficiency [%]	TOF[b] [min^{-1}]	TMBQ selectivity [%]
1	MIL-125-M	0.4	56	28	1.4	100
2	MIL-125_NH_2	0.4	50	25	1.0	100
3	MIL-125-M[c]	0.4	57	29	1.5	100
4	MIL-125-M[d]	0.4	54	27	1.3	100
5	MIL-125-M[e]	0.4	57	29	1.1	100
6	MIL-125-M	0.25	40	32	0.7	100
7	MIL-125-M	0.8	70	18	1.5	100
8	MIL-125-M	0.4[f]	35	10	n.d.[g]	57[h]
9[i]	MIL-125-M	0.4	50	24	0.1	94
10	MIL-125-M	0.25[j]	50	38	0.9	96
11	MIL-125-S	0.25[j]	49	37	1.0	96
12	MIL-125-L	0.25[j]	50	39	1.0	98
13	MIL-125_NH_2	0.25[j]	50	32	0.8	89
14	TiO_2 (Degussa P25)[k]	0.4	23	9	0.03	80[h]

[a] Reaction conditions: TMP (0.1 M), MIL-125 (3 mg), H_2O_2 (used as 35% aq. solution, 0.25–0.8 M, 44–140 µL), MeCN (2 mL), 80 °C, 10–15 min. [b] TOF = (mol of TMP consumed)/[(mol of Ti) × time]; determined from the initial rates of TMP consumption under the assumption that all Ti centers are accessible. [c] Before the catalytic reaction the catalyst was pre-heated at 130 °C under vacuum for 6 h. [d] MIL-125 (1.5 mg); reaction time 20 min. [e] MIL-125 (6 mg). [f] H_2O_2 was added dropwise over 30 min; reaction time 1 h. [g] Not determined. [h] The main byproduct was 2,2′,3,3′,5,5′-hexamethyl-4,4′-biphenol. [i] 40 °C, 4 h. [j] 88% H_2O_2 was used. [k] TiO_2 (3 mg) contained mostly anatase.

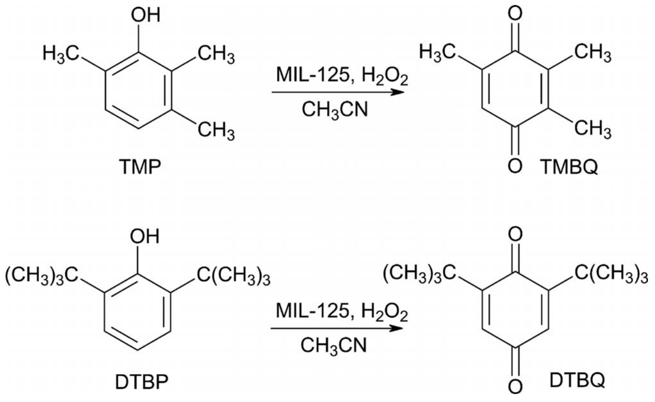

and DTBQ realized over MIL-125 is from the specific structure of MIL-125 being composed of well-defined titanium oxo-hydroxo clusters. The lack of isolated Ti species or anatase microcrystallites in the Ti-MOFs ensures the 100% *p*-benzoquinone selectivity.

Previously, some of us found that turnover frequencies (TOFs) for silica-grafted Ti catalysts with di(oligo)meric Ti centers usually vary over the range 1.4–2.1 min^{-1} for TMP oxidation.[10b] If we compare these values with TOFs characteristic of MIL-125 under the same reaction conditions (e.g., Table 2, entry 1), we can conclude that the rate of TMP oxidation, referring to one Ti center, is quite similar for both types of catalysts. Coupled with the 100% selectivity toward TMBQ, this indicates a similar structure and accessibility of the active Ti centers, at least, at the initial stage of the reaction. The presence of amine groups in the MOF linker did not affect the quinone selectivity but slightly reduced the catalytic activity (TOF 1.0 min^{-1} vs. 1.4 min^{-1} for MIL-125). The fact that microporous Ti-MIL-125 (5–7 Å windows) and mesoporous Ti,Si catalysts with pores in the range of 2.6–15.4 nm[10b] revealed close TOF values in the TMP oxidation was quite surprising for us. Previously, it was found that microporous titanium silicalite TS-1 (5.4 × 5.6 Å) is, at least, an order of magnitude less active in this reaction than mesoporous Ti,Si catalysts.[15]

In order to elucidate the impact of internal diffusion in the case of MIL-125, samples with different sizes of crystallites (0.5, 1.5, and 5 µm) have been examined. As one can judge from the kinetic curves shown in Figures S6a and b in the SI, the initial rate of both TMP and DTBP oxidation was not affected by the size of the crystallites. Therefore, we might assume that no diffusion limitation takes place in the course of the catalytic oxidation of TMP and DTBP over MIL-125, although the smallest dimensions of the TMP (5.4 × 6.7 Å) and DTBP (5.6 × 9.4 Å) molecules are close to the dimensions of the MOF cage windows. We might suppose that π–π interactions between aromatic rings of phenols and of the MOF linker (bdc) could favor efficient adsorption of the organic substrates within MIL-125, thus ensuring its high catalytic activity. Moreover, it has been recently established for hydrocarbon–zeolite systems that penetration of guest molecules into host pores can be accelerated when dimensions of guest and host are close to each other (the so-called levitation effect).[16] Similar effects were suggested for encapsulation of iron tetrasulfophthalocyanine (ca. 17 × 17 Å) into cages of Cr-MIL-101 (15 × 16 Å windows).[17] Finally, we should also take into account that destruction of the MIL-125 framework under the conditions of liquid-phase oxidation with aqueous H_2O_2 (see below) could be, at least, partially responsible for the unusually high catalytic activity of the Ti-MOFs in the selective oxidation of the alkyl-substituted phenols.

Regardless of the high activity, only moderate TMP conversions were attained for both MIL-125 and its amine-functionalized analog (56 and 50%, respectively) when a twofold excess of 35% H_2O_2 was employed. With DTBP, the substrate conversion was even lower (ca. 20%). Neither phenol conversion nor the quinone-product yield could be improved by increasing the reaction time. Preliminary treatment of MIL-125 under vacuum at 130 °C had almost no effect on the catalytic performance of the coordination polymer (Table 2, compare entries 1 and 3), which is not surprising if we remember that the structure of MIL-125 does not allow formation of coordinatively unsaturated metal sites.[5]

In principle, two main reasons for the low phenol conversions over the Ti-MOFs could be envisaged. The first reason might be blockage of the MOF pores or active sites by the reaction products during the reaction course. To investigate such a possibility, we studied the effect of the catalyst amount on the reaction course. If pore filling by oxidation products occurred, one might expect an increase of the substrate conversion upon increasing the catalyst loading. However, this parameter turned out to produce practically no effect on the resulting phenol conversion (Table 2, compare entries 1, 4, and 5).

Another reason for the low phenol conversions could be high rates of the unproductive decomposition of H_2O_2 relative to the rates of the TMP oxidation over the Ti-MOFs, i.e. a rather low efficiency of the oxidant utilization. Indeed, Figure S7 (see SI) shows that H_2O_2 decomposition occurs with a rate comparable to the rate of TMP oxidation. Iodometric titration confirmed that no H_2O_2 was present at the end of the catalytic reactions (Table 2, entries 1–6). Importantly, TMP conversion could be increased up to 97% without loss of TMBQ selectivity by using an additional portion of the oxidant (Figure 4), which proves that decomposition of H_2O_2 to produce O_2 and water is the main reason for the incomplete phenol conversions in the presence of MIL-125. However, the higher the concentration of H_2O_2 that was employed the lower the efficiency of the oxidant utilization (Table 2, compare entries 1, 6, and 7). A dropwise addition of the oxidant (this procedure is often employed to improve the oxidant efficiency) resulted in a significant decrease of both TMBQ selectivity and H_2O_2 efficiency (Table 2, entry 8). Reduction of the reaction temperature produced a similar effect, although not so pronounced (Table 2, entry 9). In general, the oxidant efficiency for the Ti-MOFs was inferior to that observed for Ti,Si catalysts, for which this parameter attained ca. 57%, i.e. a twofold excess of H_2O_2 was sufficient to convert 100% of TMP.[10b] On the other hand, both MIL-125 and MIL-125_NH_2 showed much better oxidant efficiency and selectivity toward TMBQ than anatase (Table 2, entry 14).

We found that the efficiency of the oxidant utilization over MIL-125 could be improved by reducing the amount of water in the reaction mixture. With more concentrated H_2O_2 (ca. 88%), the oxidant efficiency achieved 37–39%, but the selectivity toward TMBQ and TOF slightly decreased (Table 2, entries 10–12). Again, the size of catalyst particles produced almost no effect on the reaction rate and selectivity, indicating an insignificant role of diffusion limitations during the oxidation process.

We also attempted to use an anhydrous H_2O_2–urea adduct instead of aqueous H_2O_2. However, this led to a drastic decrease in the catalyst activity (only 4% TMP conversion under the conditions of entry 1, Table 2). In turn, the use of TBHP (4.7 M solution in decane) as the oxidant resulted in the reduction of both substrate conversion (18% after 1 h) and quinone selectivity (56% vs. 100% with H_2O_2).

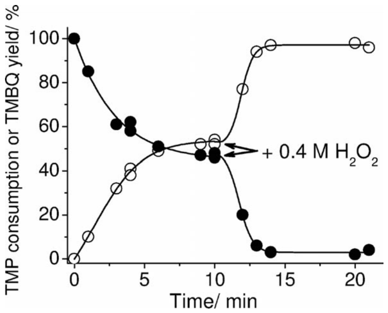

Figure 4. Effect of the oxidant amount on TMP oxidation with H_2O_2 over MIL-125-M (filled and open symbols correspond to substrate consumption and product yield, respectively). Reaction conditions: TMP (0.1 M), H_2O_2 (0.4–0.8 M, 70–140 µL), MIL-125-M (3 mg), MeCN (2 mL), 80 °C.

Catalyst Stability and Recycling

Catalyst stability toward leaching of active species and the nature of catalysis are indispensable properties of solid catalysts, which should be carefully investigated in liquid-phase oxidation processes.[18] First of all, we performed a hot filtration test and found no further substrate conversion or growth of the product yield in the filtrate after removal of the catalyst (Figure S8 in the SI). This proved that the observed catalysis in the presence of MIL-125 is truly heterogeneous, i.e. occurs on the catalyst surface rather than in solution as a result of leached active metal species. Moreover, only a trace amount of titanium (0.1 ppm) was determined in the filtrate by ICP-AES.

The MIL-125 catalyst could be recovered by simple filtration and reused without loss of selectivity to the target quinone product (Figure 5). Importantly, no catalyst regeneration was needed before reuse. In the second run, the maximal conversion of TMP and the oxidant efficiency even increased and reached 68 and 35%, respectively, while the catalytic activity expressed in TOF values determined from the initial rates of TMP consumption (the corresponding kinetic curves are given in Figure S9) decreased. However, TOFs stabilized after the second reuse (Figure 5), thus indicating that the MOF catalyst, most likely, converted to another, more stable form. It is noteworthy that the recycling behavior of the Ti-MOF catalyst in TMP oxidation is significantly better than that of mesoporous Ti,Si catalysts, for which a progressive loss of both the catalytic activity and selectivity readily occurs with 35% aqueous H_2O_2 that causes hydrolysis of Ti–O–Si bonds and agglomeration of Ti active sites on the surface.[10b]

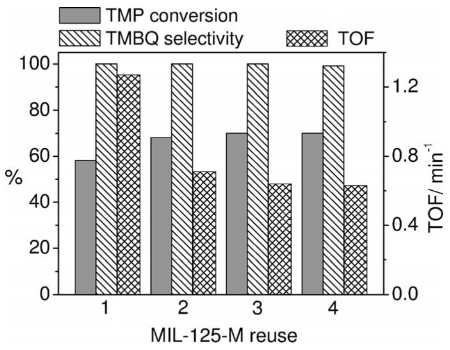

Figure 5. Reuse of MIL-125-M in TMP oxidation with 35% H_2O_2. Reaction conditions: TMP (0.1 M), H_2O_2 (0.4 M), MIL-125 (21 mg), MeCN (7 mL), 80 °C, 10 min.

Stability of the Ti-MOFs under the conditions of TMP oxidation was probed by XRD. Figure 6 shows low-angle XRD patterns of MIL-125-M before and after catalysis. The catalyst sample recovered after TMP oxidation with 35% H_2O_2 (in this case, the reaction mixture contained 1.5 M of H_2O) exhibited no XRD reflections (Figure 6, curve B), thereby indicating that the crystal structure is completely destroyed. Additionally, elemental analysis of the recycled catalyst revealed an increase of the Ti content in the MIL-125-M sample after reuse in TMP oxidation (see Table 1). A similar picture was observed for MIL-125_NH_2 although, on the basis of recent results of Ahn and coworkers,[7] one might expect a higher hydrolytic stability for the amine-modified Ti-MOF. On the other hand, after the reaction with concentrated H_2O_2 (0.1 M H_2O in the reaction mixture), the characteristic XRD reflections of MIL-125 were still present (Figure 6, curve C), even though their reduced intensity and broadening pointed at a partial decomposition and/or some local distortions of the Ti-MOF crystal structure. Obviously, structural stability of MIL-125 in liquid-phase oxidation depends on the nature of oxidant and water content in the reaction medium. Indeed, McNamara et al. demonstrated that MIL-125 was stable in the presence of TBHP even under harsh reaction conditions (24 h at 100 °C).[8]

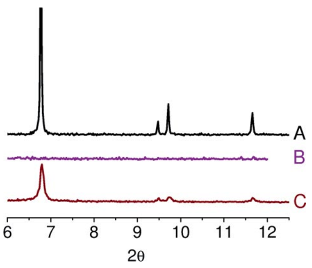

Figure 6. Low-angle XRD patterns for MIL-125-M: (A) initial, (B) and (C) after 1 run of TMP oxidation with 35 and 88% H_2O_2, respectively. Reaction conditions: TMP (0.1 M), H_2O_2 (0.4 M of 35% or 0.25 M of 88% H_2O_2), MIL-125 (21 mg), MeCN (7 mL), 80 °C, 10 min.

Both SEM and TEM images (Figures S10 and S11, respectively) showed that MIL-125-M after treatment with H_2O_2 still consisted of well-defined particles with an admixture of smaller crystallites (ca. 0.5–0.8 µm). The N_2 adsorption study on recycled MIL-125-M revealed a significant decrease of the specific surface area and appearance of mesopores instead of the initially present micropores (see Table 1; the corresponding N_2 adsorption isotherms are shown in Figure S3). We assume that the increase in TMP conversion observed in the second run (Figure 5; Figure S9) might be due to the appearance of the mesopores that favor adsorption of the phenolic substrate. Importantly, the textural parameters of the catalyst after the first and fourth reuse were very close to each other, which is in line with the observed catalytic results (Figure 5; Figure S9).

A significant broadening of signals in the FTIR spectra of recycled MIL-125 and MIL-125_NH_2 also indicated structural alterations (see Figures S4a and b in the SI, curves B–C). The IR spectra exhibited a broad absorption below 1000 cm^{-1}, which is characteristic of ionic oxides, including TiO_2 polymorphs.[14] However, it did not coincide precisely with the spectrum of any TiO_2 crystalline modification. In turn, the intensity of signals in the Raman spectra of both MIL-125 and MIL-125_NH_2 decreased markedly after the catalyst reuse (Figure 2, a and b, curves B–C), which also corroborates a MOF destruction process. However, no strong absorption bands around 140 and 160 cm^{-1} typical of TiO_2 polymorphs (anatase and brookite, respectively)[19] emerged, as one can judge from the inserts in Figure 2.

Finally, DR UV/Vis spectra of MIL-125-M recovered after the catalytic runs showed a redshift in the absorption edge and a new absorption in the visible light range (Figure 3, a, curves B and C), indicating some further agglomeration of the Ti clusters. Importantly, the DR UV/Vis spectra runs practically coincided after the first and fourth catalyst use, which, in line with the other results, implies that the main structural modification occurs during the first catalytic run to produce a new solid form that is fairly stable to further modifications. For MIL-125_NH_2, the intensity of the absorption band at 390 nm decreased after catalysis, accompanied by a redshift in the absorption edge (Figure 3, b, curve B). Note that a redshift in the absorption edge and appearance of absorption in the visible range have recently been observed for graphene-wrapped TiO_2 nanoparticles.[20] One might expect that agglomeration of TiO_2 clusters during the MOF destruction process would result in worsening the accessibility of the Ti active centers. Indeed, the initial rates normalized per one Ti atom (TOF) decreased after the first catalyst use (Figure 5).

Bearing in mind all the results collectively, we may suppose that the transformation of the MIL-125 metal–organic framework, which evidently takes place under turnover conditions of the liquid-phase oxidation with H_2O_2, has led to a stable, highly active and selective form of the catalyst, which contained amorphous fine-dispersed TiO_2, most likely, stabilized by carboxylate ions. Such stabilization did not allow the formation of anatase-like species, which are detrimental to the selective formation of benzoquinones, and might be responsible for the superior recycling performance of the MIL-125-derived catalytic material.

Conclusions

The Ti-containing metal–organic frameworks MIL-125 and MIL-125_NH$_2$ demonstrate superior selectivity toward *p*-benzoquinones in the oxidation of alkyl-substituted phenols with aqueous H_2O_2, MIL-125 being slightly more active than its amine-modified analog. With both Ti-MOFs nearly 100% selectivity was reached in the oxidation of TMP to TMBQ (vitamin E key intermediate). The efficiency of the oxidant utilization with MIL-125 and MIL-125_NH$_2$ is superior to that found for anatase (besides, the latter was significantly less selective toward the formation of benzoquinones) but inferior to the oxidant efficiency achieved previously with mesoporous titanium-silicate catalysts. The XRD, N_2 adsorption, and spectroscopic studies revealed that, under turnover conditions of the liquid-phase oxidation process, the structure of the Ti-MOFs undergoes transformation into an X-ray amorphous mesoporous solid that contains fine-dispersed amorphous TiO_2, most likely, stabilized by carboxylate ions. Such stabilization prevents the formation of anatase microcrystallites, the presence of which is detrimental to selective oxidations with hydrogen peroxide. As a result, the recycling performance of the MIL-125-derived catalytic materials is superior to that of mesoporous Ti,Si catalysts, which usually lose their activity and selectivity in the title reaction due to gradual aggregation of TiO_2 active species on the silica surface. Both the structural stability of MIL-125 and efficiency of H_2O_2 utilization over MIL-125 can be improved by reducing the concentration of water in the reaction mixture. An alternative route could be the use of a more hydrophobic organic linker for synthesis of Ti-cluster-containing MOFs.

Experimental Section

Materials: Hydrogen peroxide was used as a 35% or 88% solution in water; its concentration was determined by iodometric titration. Acetonitrile was dried and stored over activated molecular sieves (4 Å). All other reactants were obtained commercially and used without further purification.

Instrumentation: GC analyses were performed using a gas chromatograph "Tsvet-500" equipped with a flame ionization detector and a quartz capillary column (30 m × 0.25 mm) Supelco MDN-5S. GC–MS analyses were carried out using an Agilent 7000B system with triple-quadrupole mass-selective detector Agilent 7000 and GC Agilent 7890B (quartz capillary column 30 m × 0.25 mm/HP-5ms). ATR-FTIR spectra (4000–250 cm^{-1}, 32 scans, resolution 4 cm^{-1}) were collected using a Cary 660 FTIR spectrometer (Agilent Technologies) and a PIKE Technologies GladiATR accessory (diamond crystal). FT-Raman spectra (3600–100 cm^{-1}, 300 scans, resolution 4 cm^{-1}, 180° geometry) were recorded using a RFS 100/S spectrometer (Bruker). Excitation of the 1064-nm line was provided by a Nd-YAG laser (100 mW power output). DRS UV/Vis measurements were performed with a Shimadzu UV/Vis 2501PC spectrophotometer. ^{1}H NMR spectra were recorded with a Bruker Avance-400 spectrometer (400.13 MHz). Nitrogen adsorption at 77 K was studied by using an Autosorb-6B-Kr volumetric adsorption analyzer (Quantachrome Instruments, Boynton Beach, FL). Before measurements, samples were degassed at 130 °C overnight under vacuum (the final pressure was 5–6 mTorr). Specific BET surface areas (S_{BET}) were evaluated using adsorption data over a relative pressure range of 0.005 to 0.2 (P/P_0; P_0: saturation vapor pressure of N_2 at –196 °C) with a specific choice of experimental points to satisfy the consistency criteria given by Walton and Snurr.[21] The volumes of micro- and mesopores (V_{micro} and V_{meso}) were estimated by the α_S-plot method.[22] XRD measurements were performed with a high-precision X-ray diffractometer mounted on beamline No. 2 of the VEPP-3 storage ring at the Siberian Synchrotron Radiation Center (SSRC). Radiation wavelength was λ = 0.15393 nm. High natural collimation of the synchrotron radiation beam, the flat perfect crystal analyzer, and the parallel Soller slit on the diffracted beam provided an extremely high instrumental resolution of the diffractometer over a small angle region of 2θ = 0.5–10° and higher. The crystal size and morphology of the catalysts were confirmed by a scanning electron microscope (SEM, Philips, XL-30S FEG). Thermogravimetric (TG) analysis was carried out with a thermogravimetric analyzer (TA Instruments, Universal V4.5A). The TG analysis was performed in a dry nitrogen flow of 100 mL min^{-1} while the temperature was increased from 25 to 700 °C with a heating rate of 10 ° min^{-1}. To get reproducible TG data, prior to TG measurements the samples were hydrated in a chamber with 70% relative humidity at 30 °C for 1 d.

Synthesis of MIL-125 and MIL-125_NH$_2$: MIL-125 has been synthesized by a solvothermal method using terephthalic acid and titanium isopropoxide in a solvent mixture of *N*,*N′*-dimethylformamide (DMF) and methanol as reported elsewhere.[11] MIL-125_NH$_2$ was prepared using 2-aminoterephthalic acid and titanium isopropoxide in a mixture of solvents including DMF and dry methanol. The detailed preparation method is described in the SI. The particle size of samples was controlled by the addition of benzoic acid as a modulator as used for the synthesis of UiO-66[23] and the addition of water [$H_2O/Ti(OiPr)_4$ molar ratio = 1] at the initial mixing of the precursors.

Catalytic Experiments: Catalytic runs were carried out in thermostatted glass vessels under vigorous stirring at 80 °C. Typically, the reactions were initiated by adding 35% aqueous H_2O_2 (0.4 M, 70 µL) to a mixture containing TMP (0.1 M, 28 mg), MIL-125 (3 mg), internal standard (biphenyl), and acetonitrile (2 mL) as a solvent. The reaction time was 7–20 min. Samples of the reaction mixture were withdrawn periodically during the reaction course by a syringe through a septum. The reaction products were identified by GC–MS and ^{1}H NMR spectroscopic techniques and quantified by GC. Each experiment was reproduced at least three times. The experimental error in the determination of the substrate conversions and product yields normally did not exceed 2%. After reaction, the catalyst was filtered off, washed with hot acetonitrile and acetone, dried in air at room temperature, and then reused. Catalyst reusability was studied in 4–6 time-scaled experiments.

2,3,5-Trimethyl-1,4-benzoquinone (TMBQ): GC–MS (EI): *m*/*z* (relative int.) = 150 (100) $[M]^+$, 122 (47) $[M - CO]^+$, 107 (64) $[M - CO, - CH_3]^+$, 79 (48) $[M - 2CO, - CH_3]^+$. ^{1}H NMR ($CDCl_3$, 400.13 MHz, 25 °C): δ = 6.59 (s, 1 H, CH), 2.05–2.10 (m, 9 H, 3 CH_3) ppm.

2,6-Di-*tert*-butyl-1,4-benzoquinone (DTBQ): ^{1}H NMR (CD_3CN, 400.13 MHz, 25 °C): δ = 6.48 (s, 2 H), 1.26 (s, 18 H) ppm.

Supporting Information (see footnote on the first page of this article): TG profiles, XRD patterns, N_2 adsorption isotherms, FTIR and DR UV/Vis spectra, SEM and TEM images, and kinetic curves for catalytic reactions.

Acknowledgments

The authors thank Dr. I. E. Soshnikov for ^{1}H NMR measurements and Dr. M. S. Melgunov for discussions. Korean authors are grateful to Global Frontier Center for Hybrid Interface Materials (GFHIM) and ISTK for their financial support through the Global Frontier R&D Program and the Institutional Collaboration Research Program (SK-1301). The research was partially supported by the Russian Foundation for Basic Research (grant number 13-03-00413).

---

[1] a) S. Kitagawa, R. Kitaura, S. Noro, *Angew. Chem.* **2004**, *116*, 2388; *Angew. Chem. Int. Ed.* **2004**, *43*, 2334–2375; b) G. Férey, *Chem. Soc. Rev.* **2008**, *37*, 191–214; c) A. U. Czaja, N. Trukhan, U. Müller, *Chem. Soc. Rev.* **2009**, *38*, 1284–1293; d) A. Corma, H. García, F. X. Llabrés i Xamena, *Chem. Rev.* **2010**, *110*, 4606–4655; e) A. Dhakshinamoorthy, M. Alvaro, H. García, *Catal. Sci. Technol.* **2011**, *1*, 856–867; f) *Metal–Organic Frameworks Applications from Catalysis to Gas Storage* (Ed.: D. Farrusseng) Wiley-VCH, Weinheim, Germany, **2011**; g) M. Ranocchiari, J. A. van Bokhoven, *Phys. Chem. Chem. Phys.* **2011**, *13*, 6388–6396.

[2] M. Y. Masoomi, A. Morsali, *Coord. Chem. Rev.* **2012**, *256*, 2921–2943.

[3] a) A. Corma, H. García, *Chem. Rev.* **2002**, *102*, 3837–3892; b) M. G. Clerici, in: *Metal Oxide Catalysis*, vol. 2 (Eds.: S. D. Jackson, J. S. J. Hargreaves), Wiley-VCH, Weinheim, Germany, **2009**, p. 705–754; c) B. Notari, *Adv. Catal.* **1996**, *41*, 253–334; d) A. Tuel, L. G. Hubert-Pfalzgraf, *J. Catal.* **2003**, *217*, 343–353; e) M. G. Clerici, *Top. Catal.* **2000**, *13*, 373–386; f) P. Ratnasamy, D. Srinivas, H. Knozinger, *Adv. Catal.* **2004**, *48*, 1–169.

[4] M. Dan-Hardi, C. Serre, T. Frot, L. Rozes, G. Maurin, C. Sanchez, G. Férey, *J. Am. Chem. Soc.* **2009**, *131*, 10857–10859.

[5] C. Zlotea, D. Phanon, M. Mazaj, D. Heurtaux, V. Guillerm, C. Serre, P. Horcajada, T. Devic, E. Magnier, F. Cuevas, G. Férey, P. L. Llewellyn, M. Latroche, *Dalton Trans.* **2011**, *40*, 4879–4881.

[6] a) Y. Horiuchi, T. Toyao, M. Saito, K. Mochizuki, M. Iwata, H. Higashimura, M. Anpo, M. Matsuoka, *J. Phys. Chem. C* **2012**, *116*, 20848–20853; b) Y. Fu, D. Sun, Y. Chen, R. Huang, Z. Ding, X. Fu, Z. Li, *Angew. Chem.* **2012**, *124*, 3420–3423.

[7] S.-N. Kim, J. Kim, H.-Y. Kim, H.-Y. Cho, W.-S. Ahn, *Catal. Today* **2013**, *204*, 85–93.

[8] N. D. McNamara, G. T. Neumann, E. T. Masko, J. A. Urban, J. C. Hicks, *J. Catal.* **2013**, *305*, 217–226.

[9] a) P. Schudel, H. Mayer, O. Isler, in: *The Vitamins*, vol. 5 (Eds.: W. H. Sebrell, R. S. Harris), Academic Press, New York, **1972**, p. 165; b) *The Chemistry of Quinonoid Compounds* (Eds.: S. Patai, Z. Rappoport), Wiley-Interscience, New York, **1988**; c) W. Bonrath, M. Eggersdorfer, T. Netscher, *Catal. Today* **2007**, *121*, 45–57.

[10] a) O. A. Kholdeeva, I. D. Ivanchikova, M. Guidotti, N. Ravasio, *Green Chem.* **2007**, *9*, 731–733; b) O. A. Kholdeeva, I. D. Ivanchikova, M. Guidotti, C. Pirovano, N. Ravasio, M. V. Barmatova, Y. A. Chesalov, *Adv. Synth. Catal.* **2009**, *351*, 1877–1889; c) O. A. Kholdeeva, I. D. Ivanchikova, M. Guidotti, N. Ravasio, M. Sgobba, M. V. Barmatova, *Catal. Today* **2009**, *141*, 330–336.

[11] F. Vermoortele, M. Maes, P. Z. Moghadam, M. J. Lennox, F. Ragon, M. Boulhout, S. Biswas, K. G. M. Laurier, I. Beurroies, R. Denoyel, M. Roeffaers, N. Stock, T. Düren, C. Serre, D. E. De Vos, *J. Am. Chem. Soc.* **2011**, *133*, 18526–18529.

[12] a) X. Gao, I. E. Wachs, *Catal. Today* **1999**, *51*, 233–254; b) N. N. Trukhan, V. N. Romannikov, A. N. Shmakov, M. P. Vanina, E. A. Paukshtis, V. I. Bukhtiyarov, V. V. Kriventsov, I. Yu. Danilov, O. A. Kholdeeva, *Microporous Mesoporous Mater.* **2003**, *59*, 73–84.

[13] a) L. Marchese, T. Maschmeyer, E. Gianotti, S. Coluccia, J. M. Thomas, *J. Phys. Chem. B* **1997**, *101*, 8836–8838; b) L. Marchese, E. Gianotti, V. Dellarocca, T. Maschmeyer, F. Rey, S. Coluccia, J. M. Thomas, *Phys. Chem. Chem. Phys.* **1999**, *1*, 585–592.

[14] B. J. Aronson, C. F. Blanford, A. Stein, *Chem. Mater.* **1997**, *9*, 2842–2851.

[15] O. A. Kholdeeva, M. S. Melgunov, A. N. Shmakov, N. N. Trukhan, V. V. Kriventsov, V. I. Zaikovskii, M. E. Malishev, V. N. Romannikov, *Catal. Today* **2004**, *91–92*, 205–209.

[16] H. Jobic, B. J. Borah, S. Yashonath, *J. Phys. Chem. B* **2009**, *113*, 12635–12638.

[17] O. V. Zalomaeva, K. A. Kovalenko, Yu. A. Chesalov, M. S. Mel'gunov, V. I. Zaikovskii, V. V. Kaichev, A. B. Sorokin, O. A. Kholdeeva, V. P. Fedin, *Dalton Trans.* **2011**, *40*, 1441–1444.

[18] R. A. Sheldon, M. Wallau, I. W. C. E. Arends, U. Schuchardt, *Acc. Chem. Res.* **1998**, *31*, 485–493.

[19] a) G. Busca, G. Ramis, J. M. Gallardo Amores, V. S. Escribano, P. Piaggio, *J. Chem. Soc. Faraday Trans.* **1994**, *90*, 3181–3190; b) G. A. Tompsett, G. A. Bowmaker, R. P. Cooney, J. B. Metson, K. A. Rodgers, J. M. Seakins, *J. Raman Spectrosc.* **1995**, *26*, 57–62.

[20] J. S. Lee, K. H. You, C. B. Park, *Adv. Mater.* **2012**, *24*, 1084–1088.

[21] K. S. Walton, R. Q. Snurr, *J. Am. Chem. Soc.* **2007**, *129*, 8552–8556.

[22] S. J. Gregg, K. S. W. Sing, *Adsorption, surface area and porosity*, Academic Press, New York, **1982**.

[23] A. Schaate, P. Roy, A. Godt, J. Lippke, F. Waltz, M. Wiebcke, P. Behrens, *Chem. Eur. J.* **2011**, *17*, 6643–6651.

Received: August 26, 2013